Adsorption of Pb(II) by montmorillonite modified biochars and reduction Pb(II)-stress in plants of microcosms of constructed wetlands: mechanism and treatment performances

Yaohong Zhang[a,b,†], Renrong Liu[a,†], Liya Tan[a], Ningcan Yang[a], Anna Kerkula[a], Hai Wang[a,*]

[a]School of Life Science, School of Chemistry and Chemical Engineering, Shaoxing University, Shaoxing 312000, China,
emails: wanghai@usx.edu.cn/wanghai2243@126.com (H. Wang), zhangyhsxu@126.com (Y. Zhang), 1124131057@qq.com (R. Liu),
799832811@qq.com (L. Tan), 846778861@qq.com (N. Yang), annakerkula@yahoo.com (A. Kerkula)
[b]Zhejiang Key Laboratory of Alternative Technologies for Fine Chemicals Process, Shaoxing 312000, China

ABSTRACT

In the study, the peanut shell was selected as original biochar and modified by adding montmorillonite to obtain modified biochar (B@M). The adsorbent was characterized by scanning electron microscopy, Brunauer–Emmett–Teller, Fourier-transform infrared spectroscopy and X-ray diffraction. The adsorption kinetics study of Pb(II) on B@M showed that the adsorption process of Pb(II) was according to the pseudo-second-order model and Langmuir adsorption model. The maximum adsorption capacity of B@M (61.5 mg g^{-1}) was significantly higher than that of the biochar (35.5 mg g^{-1}) and montmorillonite (54.4 mg g^{-1}) and the reproducibility study indicated that B@M had good reproducibility. When the B@M was added to the microcosms of constructed wetlands (MCW), it showed that with the increase of the amount of B@M, the removal rate of lead in water increased significantly, which was 31.3%, 48.3% and 86.1%, respectively and can reduce the stress of Pb(II) in plants of MCW. Therefore, B@M can be used as a new substrate material and heavy metal Pb(II) adsorbent for constructed wetlands.

Keywords: Modified biochars; Constructed wetland; Pb(II); Plant; Stress

1. Introduction

Currently, untreated sewage containing heavy metals is a serious universal problem. In the industrial processes of mining, smelting, processing, electroplating, etc., the wastewater has not been treated effectively [1], resulting in serious levels of heavy metals in water. The main hazards of heavy metals are toxicity, durability and accumulation [2]. So, metal ions should be removed from wastewater before reusing for agricultural purposes. Pb(II) is one of the main heavy metals and is harmful to biological health [3,4]. At present, the main methods of heavy metal treatment of untreated sewage are chemical, membrane filtration, reverse osmosis and adsorption [1,5]. Among them, adsorption is the most widely used method because of its simplicity, rapid and high-efficiency [6]. The emerging adsorbents have been studied that hollow Fe$_3$O$_4$@PDA nanoparticles [7], Cu@Graphitic carbon [8] and Go [9]. Hence, the shortcomings of the prohibitive cost, complex preparations are limited their application and development. Therefore, it is highly desirable to develop much cheaper, and more efficient water-absorbing agents to be used in the treatment of sewage.

Biochar is produced from the pyrolysis of agriculture wastes at a high temperature with an oxygen-limited

---

* Corresponding author.

† These authors contributed equally to this work.

atmosphere, which has the advantage of easy available and low-cost [10,11]. Biochar have dense porous materials, abundant organic oxygen-containing functional groups and high ion-exchange capacity [2], which is beneficial to the adsorption of heavy metal from raw sewage. The adsorption capacities of biochars from different raw materials are naturally reformed. Many factors affect the adsorption efficiency of heavy metals, such as pyrolysis temperature, pH value, reaction temperature, and modification [12]. Hence, some original biochars has low adsorption rates for heavy metal, which limits the application of biochar [13]. The determinants of improving the adsorption capacity of biochar are raw materials and modification processes [12]. Thus through modification can significantly improve the adsorption capacity of biochar. Clay's minerals are a part of the earliest developed adsorbents [14]. Yao et al. [15] developed material for adhering clay minerals to the surface of biochar. It was noted that clay minerals enlarged the adsorption capacity of biochar to methylene blue. The adsorption is mainly ion-exchange (clay minerals) and electrostatic interaction (biochar). These studies showed that clay minerals have definite potential for the modification of biochar [15,16]. Therefore, clay mineral montmorillonite was selected to modify the original biochar in the work.

Peanut shell was a cheap and usable solid agricultural waste, which was chosen as the main raw material for biochar. The biochar was prepared at 523 K and modified with montmorillonite. The adsorption capacity of composite materials for heavy-metal Pb(II) in water was studied, and the adsorption mechanism was discussed. After all, modified biochar (B@M) with good adsorption capacity was applied to microcosms of constructed wetlands (MCW, Fig. 1). The potential applications of biochar as a growth medium in hydroponic systems [17–19] or as a safeguard against the harmful effects of pollutants [17,19] have been investigated previously and the studies indicated that biochar with good adsorption capacity can reduce the toxic stress of heavy metal on hydroponic plants [19]. Other studies of constructed wetlands have demonstrated that the use of biochar from wood, bamboo and corn cobs can improve its ability to remove biochemical oxygen demand (BOD_5), total suspended solids [20,21], total nitrogen, total phosphorus and NH_4^+–N [21–26]. However, few studies have investigated the performance of biochar (different dosages of B@M, and recycled B@M) for MCW treating Pb(II) in wastewater.

The principal contents of this study were divided into two parts. The first part included: (1) Composite materials of B@M from peanut shell were prepared at 523 K and were characterized by Brunauer–Emmett–Teller (BET), scanning electron microscopy (SEM), Fourier-transform infrared spectroscopy (FTIR) and X-ray diffraction (XRD). (2) The effects of different adsorption conditions (pH values, temperature and solution concentration) on the adsorption of Pb(II) in water by B@M from peanut shell were studied. In addition, after the above adsorption research, the application of B@M in MCW was studied. The main contents included effects of different dosages of B@M and recycled B@M on adsorption of Pb(II), plant growth, plant biomass, tissue Pb(II) concentration and tissue Pb(II) accumulation.

2. Material and methods

2.1. Preparation of biochar and characterization

The peanut shell collected from Shaoxing City, Zhejiang Province, China was used as the original material. After washing with deionized water, the peanut shells were dried in nature to remove the deionized water. The biochar was burned under oxygen-limited conduction at a pyrolysis temperature of 523 K for 2 h, and after natural cooling, it was pulverized and screened. Clay mineral montmorillonite was added to the biochar in a weight ratio
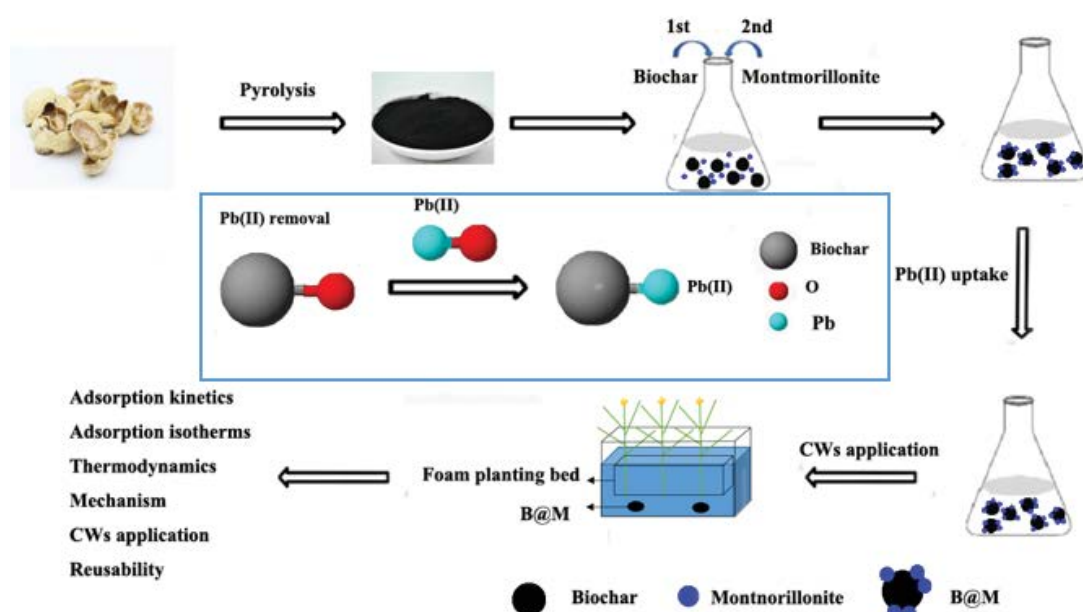

Fig. 1. Preparation of B@M, removal Pb(II) and application in MCW.

of 1:1.5, stirred in a deionized water environment for 2 h at 4,500 rpm with a magnetic agitator, and dried at 378 K. Then we can get the modified biochar (B@M).

The surface morphology of B@M was observed by scanning electron microscope (SEM); the elemental analysis was carried out by an elemental analyzer. The specific surface area and microporous structures were determined by the specific surface area (N_2-BET) and porosity tester; the surface functional groups were qualitatively analyzed by FTIR and the crystal structure and phase were determined by X-ray diffractometer (XRD).

2.2. Adsorption experiment of Pb(II)

To analyze the effect of contact time and solution pH values on the adsorption, adding 50 mg absorbent into the 100 mL 50 mg L^{-1} Pb(II) solution at 150 rpm (T = 298 K). The solution pH values were adjusted to 2.0–6.0 by using low concentration HCl or NaOH solutions. Within the specified time, the adsorbed solution was filtered and separated. The samples were taken in a 25 mL colorimetric tube, and a certain amount of 8-hydroxyquinoline (HOz) solution, sodium hydroxide solution, sodium sulfite solution, T(DBHP)P solution and emulsifier OP solution were added in sequence, and deionized water was added to the calibration line. The final step was to shake. The concentration of Pb(II) was determined by inductively coupled plasma-atomic emission spectroscopy (ICP-AES) (Perkin-Elmer Plasma 3200, Waltham, Massachusetts, USA) [17,19]. At 479 nm, the absorbance at the corresponding time was measured by a 1 cm colorimetric dish with a similar reagent blank as the reference. Finally, the difference in concentration before and after adsorption was compared. In addition, all chemicals used were of analytical grade and dissolved in deionized water during the study. After the adsorption of Pb(II) ions, the recycled B@M desorption by 1 M HNO_3 [27] was used for subsequent research of MCWs.

2.3. Experiment in microcosms of constructed wetlands

2.3.1. Experimental design

The experiment was carried out in the greenhouse of Environmental Science Department, Shaoxing University, China (29°59′N, 120°34′E). The average daily temperature of the greenhouse was in the range of 20°C–23°C and at around 20°C (night), and the humidity was maintained at 65%–80%. In early April, cultivate seedlings of *Iris tectorum* begun, and then uniform and vigorous seedlings were transferred from the nursery to microcosms of constructed wetlands (MCWs, length × width × depth = 50 cm × 38 cm × 18 cm per plastic tub, Fig. 2) after two weeks. A foam planting bed (42 cm length × 31 cm width × 8 cm height) with 12 spaced apart planting holes was used as a support to keep the seedlings in each microcosm. Water or nutrient solution of 15 L was supplied to each microcosm.

Plants were grown directly into Cooper's nutrient solution comprising: N(200 mg L^{-1}); P(60 mg L^{-1}); K(300 mg L^{-1}); Ca(170 mg L^{-1}); Mg(50 mg L^{-1}); S(69 mg L^{-1}); Fe(12 mg L^{-1}); Mn(2 mg L^{-1}); Cu(0.1 mg L^{-1}); Zn(0.1 mg L^{-1}); B(0.3 mg L^{-1}) and Mo(0.2 mg L^{-1}) [28] to avoid sorption of Pb(II) onto the
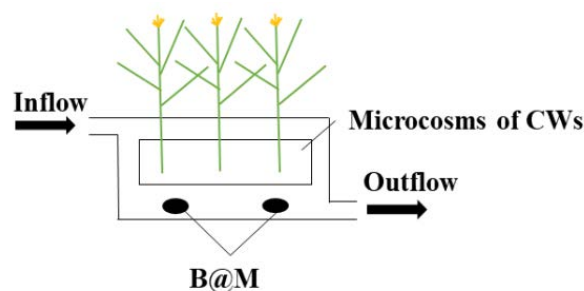

Fig. 2. Experimental system of the microcosms.

growth media [17]. The pH value of the nutrient solution was set to 5.5 by using a low concentration of HCl or NaOH. To ensure the growth of the plants, an air pump was used to supply oxygen to the root zone. After 6 d, microcosms were placed into six treatments: T_1: plants only, no Pb(II), T_2: plants containing 100 μM Pb(II) but no biochar, T_3: plants containing 100 μM Pb(II) and 0.5 g B@M, T_4: plants containing 100 μM Pb(II) and 1.0 g B@M, T_5: plants containing 100 μM Pb(II) and 4.0 g B@M, and T_6: plant containing 100 μM Pb(II) and 1.0 g regenerated B@M (the recycled B@M desorption by 1M HNO_3). T_1 was the control treatment, and T_2 was utilized to distinguish the toxic effect of Pb(II). T_3, T_4 and T_5, T_4 and T_6 were used to study the effects of different dosages of B@M and recycled B@M on Pb(II) adsorption and plant growth, respectively. The B@M samples were loaded into perforated cloth bags and placed in simulated constructed wetlands. The nutrient solution and tap water was renewed every 3 d, and a 100 μM $PbCl_2$ solution was added to the tap water of the T_2 to T_6 treatments. Packing of B@M was replaced with a new one with each water replacement. Wastewater samples of T_2 to T_6 were collected before and after each replacement of nutrient solution, respectively. All treatments were performed five times.

2.3.2. Plant analysis and measurement of Pb(II) in wastewater

After five weeks of sowing, plant samples were harvested from each microcosm to measure plant height and root length. Wash the roots and shoots of the plants with tap water. The samples were then dried in an oven at 65°C until completely dry and weighed. To determine Pb(II) contents in plant tissue, the plant samples were ground using an electric grinder. After digesting with a 0.5 g ground material with a mixture of HNO_3 – $HClO_4$ (3:1), the Pb(II) content was measured by flame AAS (Varian AA240FS) [29]. Plant Pb(II) accumulation (pool) was obtained by Pb(II) tissue concentrations by plant tissue biomass.

The concentration of Pb(II) in water samples of T_2 to T_6 was determined by ICP-AES (Perkin-Elmer Plasma 3200, Waltham, Massachusetts, USA). Removal rate (%) of Pb(II) was calculated as ((input–output)/input) × 100%.

2.4. Data processing and statistical analysis

2.4.1. Adsorption experiment

The adsorption removal rate and adsorption capacity of Pb(II) in water by B@M were expressed by *R* and q_e, respectively.

$$R = \left(1 - \frac{C_t}{C_0}\right) \times 100\% \qquad (1)$$

$$q_e = \left(C_0 - C_e\right)\frac{V}{m} \qquad (2)$$

where C_0 was the initial concentration of heavy metal Pb(II) in solution (mg L^{-1}); C_t was the concentration of Pb(II) in solution at t time (mg L^{-1}); C_e was the concentration of Pb(II) in solution at adsorption equilibrium (mg L^{-1}); V was the volume of Pb(II) solution (L); m was the dosage of biochar (g).

In order to avoid experimental errors, three parallel groups were established in the experiment, and the data results were processed independently and repeatedly. Experimental deviations were less than 5%. Finally, the average value was used as the measurement result. Data processing was carried out with Microsoft Excel 2007 and Origin 7.0.

2.4.2. MCW experiment

Statistical analysis of MCW experiment was performed with SPSS 18.0. Means were compared by the analysis of standard error (SE). Differences were considered significant at $p < 0.05$ based on one-way analysis of variance (ANOVA).

3. Results and discussion

3.1. Characterization of adsorbents

Table 1 was the pore structure of the studied samples by BET. As shown in Table 1, the surface area, total pore volume, and average pore width of B@M observably increased by more than 2 times, 6 times, and 3 times, respectively, that of the biochar. These indicated that montmorillonite prominent improves biochar performance. Fig. 3 shows the surface morphology and elemental composition of B@M by SEM and energy-dispersive X-ray spectroscopy (EDS). It can be seen that the surface of B@M was covered with small particles with irregular porous structure, which improved the adsorption capacity. The contact between metal ions and absorbent provided more space by the roughness of the surface and edge of the absorbent [30].

Figs. 3a and b show that when montmorillonite was mixed with biochar, montmorillonite adhered to the surface of biochar and provided sufficient morphology for the adsorption of Pb(II). The transmission electron microscopy (TEM) image (Fig. 3c) shows that the surface of B@M was massive, and there were flocculent substances on the surface.

In the EDS of Fig. 4a, biochar's main elements C and O were 68.5% and 31.4%. It also can directly see that those mineral elements of Al, Si, Ca and Fe came from montmorillonite (Figs. 4b and c). After adsorption, the Pb element adhered to B@M (Fig. 4d). It showed that Pb(II) has been

Table 1
Pore structure of the studied samples

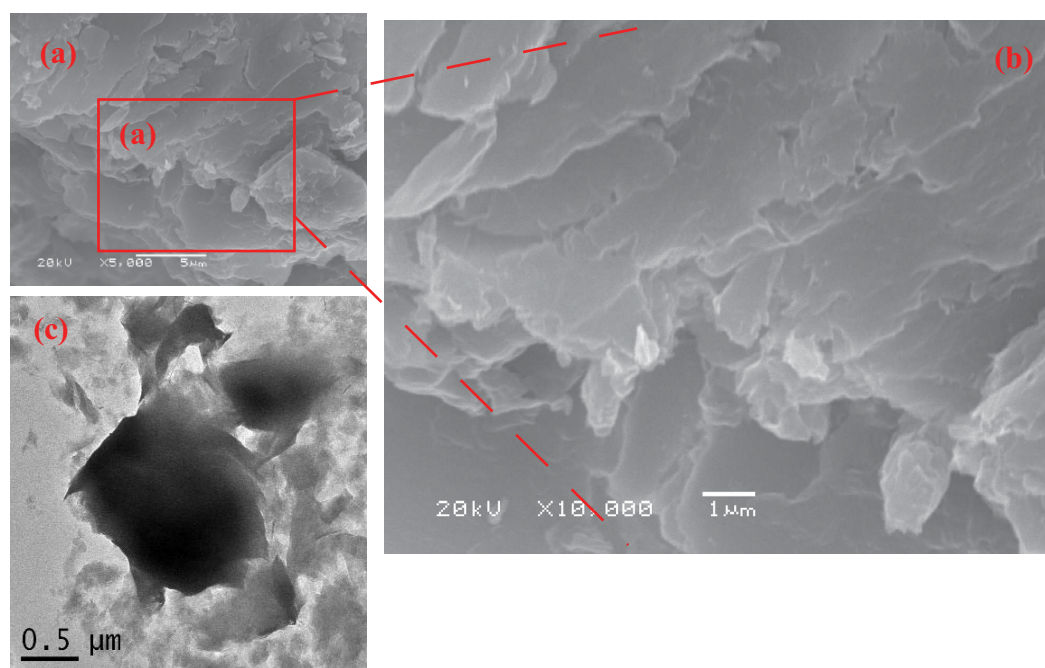| Adsorbent	BET surface area (m^2 g^{-1})	Total pore volume (cm^3 g^{-1})	Average pore width (nm)
B@M	6.18	0.020	12.7
Biochar	2.79	0.003	3.94
Montmorillonite	31.3	0.073	9.33

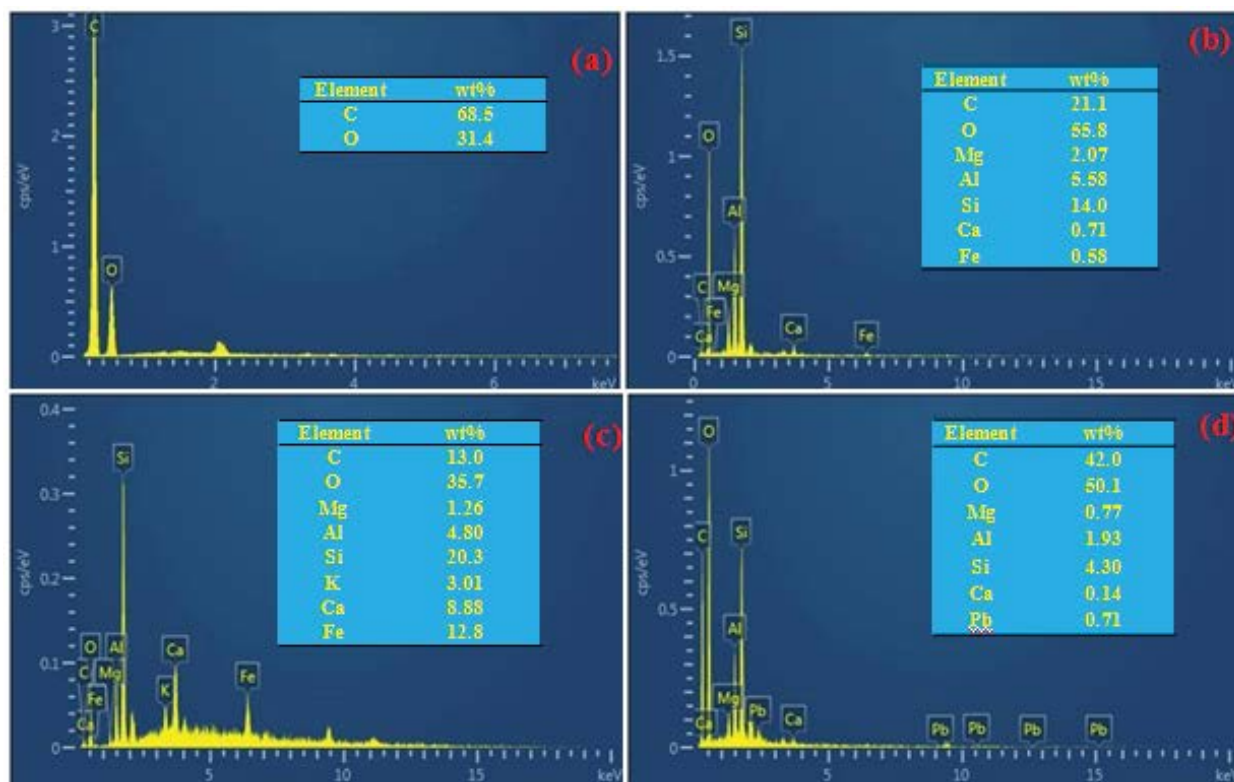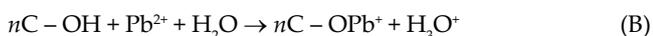Fig. 3. Characterizations of the B@M (a and b) SEM images and (c) TEM image.

Fig. 4. EDS spectrum of biochar (a), montmorillonite (b), B@M (c) and B@M-Pb(d).

adsorbed on the surface of B@M (Fig. 4d). The composition elements of biochar were similar to other biochars, which indicated that the biochar prepared at 523 K has successfully become an adsorbent [31].

From the FTIR diagram (Fig. 5), it can be revealed by the surface functional groups of adsorbents. In general, the characteristic peak around 1,180–3,698 cm^{-1} indicated that there are a series of absorption peaks in the adsorbents, such as –COOH, –OH in water molecules [32,33]. When band at near 1,137 cm^{-1}, it represented the stretching vibration of mostly C–O (including alcohols, ethers, phenols, etc.); when peak at about 1,460 cm^{-1}, it was the stretching vibration of C–H; when the characteristic peak at around 1,700 cm^{-1} assigned to the stretching vibration of C=O; when peak at 3,500–3,700 cm^{-1}, it was the stretching vibration peak of associating –OH.

The addition of montmorillonite to biochar, significantly increased the adsorption peak of 2,100 cm^{-1}, most of them were triple bonds, while the association of –OH, C–O and –COOH groups increased. The heavy metal would be complex with the surface groups of adsorbents. The reaction process was expressed by the following two equations [34].

$$nC - COOH + Pb^{2+} + H_2O \rightarrow nC - COOPb^+ + H_3O^+ \quad (A)$$

$$nC - OH + Pb^{2+} + H_2O \rightarrow nC - OPb^+ + H_3O^+ \quad (B)$$

According to the X-ray diffraction pattern (Fig. 6), the diffraction peaks near 2θ = 11° and 24.5° indicated the formation of biochar [35], and the diffraction peak at 2θ = 35° was presumed to be calcium carbonate crystal face. At the
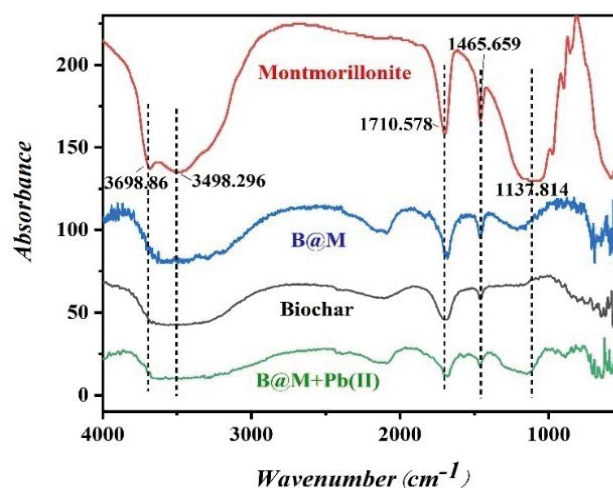

Fig. 5. FTIR diagrams of adsorbents. *Note*: B in the figure represents the diffraction peak in biochar; M is the diffraction peak in montmorillonite; B@M is peanut shell + montmorillonite biochar.

same time, it showed that no new material is produced in the synthesis process. The four new peaks at 2θ = 5.85°, 19.72°, 26.63° and 61.76° come from montmorillonite, which were d(001), d(0211), d(130) and d(060) of montmorillonite [36]. The quartz diffraction peak of biochar samples appeared at 2θ = 26°, which indicated the existence
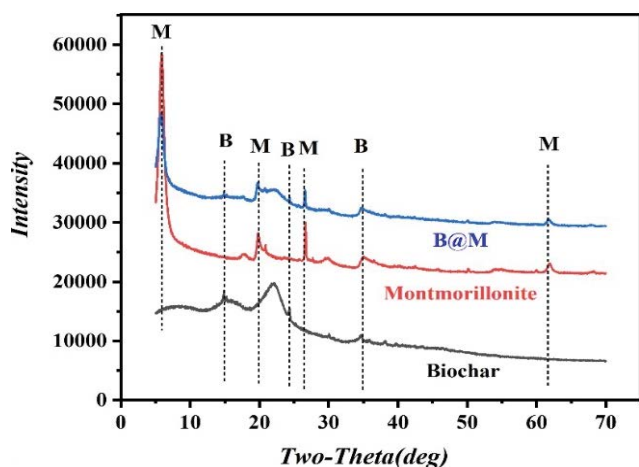
Fig. 6. XRD diagrams of adsorbents. *Note*: B in the figure represents the diffraction peak in biochar; M is the diffraction peak in montmorillonite; B@M is peanut shell + montmorillonite biochar.

Fig. 7. Removal rates of Pb(II) by B@M in different pH.

of SiO_2 in montmorillonite [37]. The SiO_2 in the adsorption materials was helpful to the adsorption of heavy metals [38].

3.2. Effect of solution pH value on adsorption of Pb(II)

The solution pH was an important factor affecting the adsorption of heavy metal ions. Under acidic conditions, plenty of hydrogen ions can inhibit the adsorption of Pb(II) by biochar [39]; once pH > 6.0, pH was greater than 6.0, Pb(II) existed in the form of $Pb(OH)_2$, from ionic state to colloidal state [40]. This also confirmed the conclusion of previous studies that the best pH of removal Pb(II) was between 4.5 and 5.5 [41,42]. This work also proved that in the pH = 5.0, the removal rate of Pb(II) reached the highest point (Fig. 7). Pb(II) existed in the form of a free state when pH < 6.0. Meanwhile, the pH of the original solution was about 5.0, so the subsequent experiment did not need to adjust the pH of the original solution.
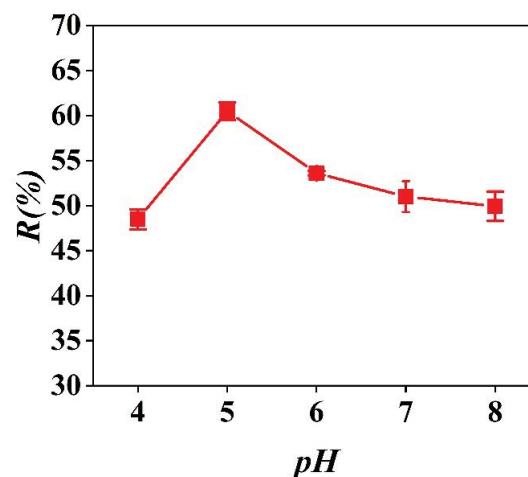
3.3. Effect of adsorbed time

From Fig. 8 it is obvious that the adsorption reaction reached equilibrium within 40 min. Meanwhile, the removal effect of B@M (61.5 mg g^{-1}) was better than the biochar (35.5 mg g^{-1}) and montmorillonite (54.4 mg g^{-1}). It indicated that B@M showed a better adsorption capacity of 61.5 mg g^{-1}.

3.4. Adsorption kinetics of Pb(II) on B@M

The adsorption mechanism of Pb(II) in solution was studied by fitting experimental data with two models: pseudo-first-order and pseudo-second-order.
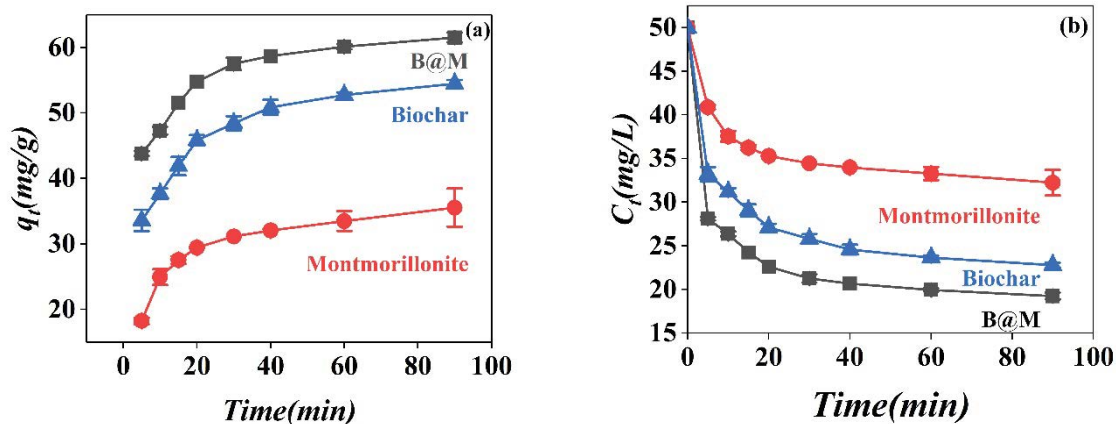
$$q_t = q_e\left(1 - e^{-k_1 t}\right) \tag{3}$$

Fig. 8. Effects of different adsorbents on the removal of Pb(II) from the solution (pH = 5.0 ± 0.2; C_0 = 50 mg/L; $V_{(Pb(II))}$ = 100 mL; temperature = 25°C).

$$\frac{t}{q_t} = \frac{1}{k_2 q_e^2} + \frac{t}{q_e} \qquad (4)$$

where t was the adsorption time (min); k_1 was pseudo-first-order model rate constant (min^{-1}); k_2 was pseudo-second-order model rate constant (min^{-1}); q_t and q_e were the amount of Pb(II) adsorbed per unit mass (mg g^{-1}) at t time and adsorption equilibrium, respectively. According to the above formulas, in the adsorption process, the important factor affecting the adsorption effect is the adsorption time [15]. Through the preliminary experiment, it was found that the adsorption equilibrium of Pb(II) on 90 min was achieved by the biochar with peanut shell as raw material, thus the final sampling time was set at 90 min.

The adsorption kinetics of Pb(II) on the biochar, montmorillonite and B@M were evaluated by the pseudo-first-order model and pseudo-second-order model. All the metal parameters are shown in Table 2. Compared to the pseudo-first-order model, the pseudo-second-order model had a better correlation which fitted the experimental data ($R^2 = 0.999$). Besides, the experiment q_e value was much closer to the calculated q_e value. Generally, the pseudo-second-order model represented the chemisorption involving valency forces [43]. Thus, this represented that the chemical process might control the overall rate of Pb(II) in the adsorption process [41].

For many adsorption, the intraparticle diffusion model was used to describe the rate-controlling step of the adsorption and analyze the existence of this process [37,44]. The related formula can be written as:

$$q_t = K_i t^{1/2} + C \qquad (5)$$

where K_i is intraparticle diffusion model rate constant (mg g^{-1} min$^{-0.5}$); C is intraparticle diffusion model rate intercept, the rate constant; t is the adsorption time (min); q_t is the amount of Pb(II) adsorbed per unit mass (mg g^{-1}) at t time.

As shown in Fig. 9, the fitting curve exhibits a multi-segment linear relationship. The first stage was the rapid adsorption process mainly occurs on the surface of biochar in the pre-adsorption period; in the second stage, the adsorption rate decreased significantly. The K_i value and C value of B@M ($k_1 > k_2$, $C_2 > C_1$) shown in Table 3, indicates that the adsorption was rapid in the first stage due to B@M's large surface area. With the passage of adsorption time, the adsorption sites on the surface of biochar decreased and the adsorption efficiency decreased.

Because the curve cannot pass through the origin ($C \neq 0$), suggesting that the intraparticle diffusion was not the only rate of the control procedure. Hence, it could still have a considerable effect on the adsorption rate [34].

3.5. Adsorption isotherm

The adsorption isotherms of Langmuir and Freundlich were selected to study the adsorption isotherms.

Langmuir equation:

$$\frac{C_e}{q_e} = \frac{1}{k_L q_m} + \frac{C_e}{q_m} \qquad (6)$$

Freundlich equation:

$$\ln q_e = \ln k_F + \frac{1}{n} \ln C_e \qquad (7)$$

Among them, C_e is the solution concentration at adsorption equilibrium (mg L^{-1}); q_e – the adsorption amount at equilibrium) (mg g^{-1}); q_m – the maximum dosage of adsorbents (mg g^{-1}); k_L – Langmuir constant), which is related to the affinity between absorbents and adsorbents. k_F is the Freundlich constant, which is related to the adsorption capacity of the adsorbents, and n was the parameter related to the interaction strength between the adsorption molecules and the surface of the adsorbents.

The adsorption isotherms of Pb(II) by B@M are shown in Fig. 10. As shown in Fig. 10, the Pb(II) adsorption capacity of
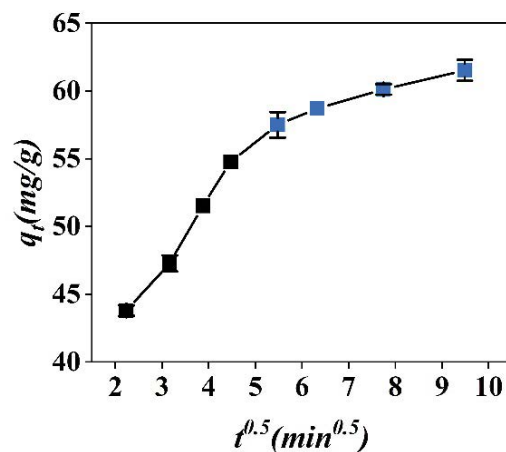
Fig. 9. The intraparticle diffusion curve of Pb(II) by B@M.

Table 2
Kinetic parameters of Pb(II) adsorption on diverse sorbents under specified circumstances (pH = 5.0 ± 0.2; T = 298 K; $C_{\text{Pb(II)initial}}$ = 50 mg L^{-1}; m(sorbent) = 0.05 g)

Adsorbent	$q_{e,\text{exp}}$	Pseudo-first-order parameter			Pseudo-second-order parameter		
		q_e	k_1	R^2	q_e	k_2	R^2
B@M	61.5	20.0	0.047	0.98	63.3	0.005	**0.99**
Biochar	35.5	9.04	0.007	0.94	37.2	0.005	**0.99**
Montmorillonite	54.5	24.6	0.046	0.99	57.1	0.004	**0.99**

Table 3
Parameter of intraparticle diffusion for Pb(II) on B@M (pH = 5.0 ± 0.2; C_0 = 10 mg L^{-1}; m(adsorbent) = 0.05 g)

Adsorbent	First stage			Second stage		
	k_1	C_1	R^2	k_2	C_2	R^2
B@M	3.49	40.5	0.99	1.35	56.1	0.99

B@M increased with the increase of adsorption equilibrium concentration and temperature. The parameter of adsorption isotherm of Pb(II) adsorption are listed in Table 4. The data fitting results of adsorption isotherm model indicated that the Langmuir model was considered to be more reliable due to it has higher R^2 values (0.98–0.99). In addition, Langmuir model described that the maximal adsorption capacity (q_m) of B@M (20°C) < B@M (30°C) < B@M (40°C), which showed that this adsorption was an endothermic process.

As shown in Table 5, the obtained thermodynamic parameters can describe the thermodynamic of adsorption [37]. The values of $\Delta G°$ were negative values, indicating that the adsorption process was spontaneous. And the values of $\Delta G°$ became more negative, suggesting that B@M has more adsorption capacity at the higher temperature. The $\Delta H°$ ($\Delta H° > 0$) mean that the adsorption of B@M was an endothermic process. And B@M and Pb(II) had a strong interaction in the adsorption process. According to the positive values of $\Delta S°$, B@M had an endothermic affinity for Pb(II).

3.6. Reusability

To test the reusability of B@M for removal Pb(II) in solution, the adsorption and desorption experiments were carried out for five times. The B@M was rinsed by 100 mL of 0.1 mol L^{-1} NaOH, then rinsed by 100 mL of 0.01 mol L^{-1} HCl for 30 min, and washed with distilled water again for 5 min. Thus treated B@M was used as adsorbents for the recycling experiments. The repeated reusability of B@M is shown in Fig. 11. From Fig. 11 it can be concluded that the removal rate of Pb(II) decreased from 61.5% to 49.2% during five adsorption and desorption experiments. It shows that the chemical stability of B@M was very well.

3.7. Application in microcosms of constructed wetlands

A case study of microcosms of constructed wetlands (MCW) was performed to evaluate the applicability of B@M. The effects of different dosages of B@M and recycled B@M on adsorption of Pb(II) ion, plant growth, plant biomass, tissue Pb(II) concentration and tissue Pb(II) accumulation were investigated.

As shown in Table 6 and Fig. 12, among the six different treatment, T_1 (the control, no Pb(II) addition) plants had the best growth, with the highest plant height, root length, aboveground biomass, underground biomass and R/S rate, because they were not subjected to Pb(II)-stress. It can be seen from T_3, T_4 and T_5, with the increasing addition of B@M, Pb(II) content in both aboveground and underground parts of plants significantly reduced ($P < 0.05$),

Table 5
Thermodynamic parameters for Pb(II) adsorption on B@M

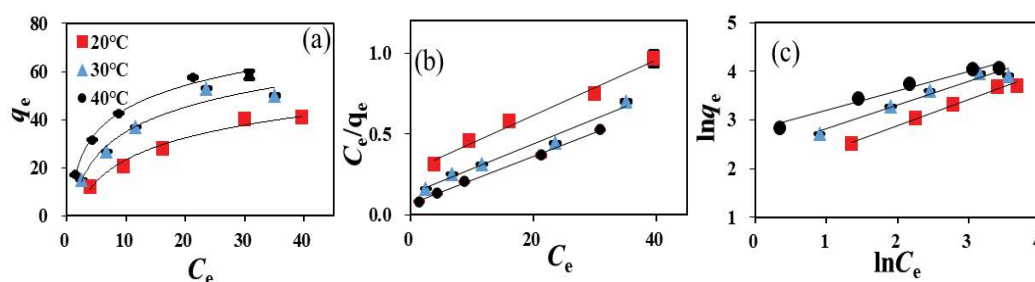| T (°C)	K	$\Delta G°$ (kJ mol^{-1})	$\Delta H°$ (kJ mol^{-1})	$\Delta S°$ (kJ mol^{-1} K^{-1})
20	1.60	−1.22		
30	3.06	−2.81	1.58	19.2
40	6.13	−4.41		

Fig. 10. Removal effect of Pb(II) by B@M at different reaction temperatures.

Table 4
Parameters of adsorption isotherm of Pb(II) adsorption (pH = 5.0 ± 0.2; m(adsorbent) = 0.05 g)

T (°C)	Langmuir adsorption model				Freundlich adsorption model		
	q_m (mg g^{-1})	k_L (L mg^{-1})	R^2	R_L	k_F	n	R^2
20	58.5	0.06	**0.99**	0.62	10.4	3.27	0.93
30	64.5	0.12	**0.98**	0.45	13.1	3.24	0.89
40	68.0	0.22	**0.99**	0.32	14.8	3.32	0.90

Table 6
Effects of different treatments on plants in constructed wetlands

Treatments	Plant height (cm)	Root length (cm)	Aboveground biomass (g plant⁻¹)	Underground biomass (g plant⁻¹)	R/S
T_1	43.8 ± 4.22a	18.5 ± 2.12a	7.06 ± 1.11a	6.87 ± 1.89a	0.97
T_2	31.6 ± 3.21c	12.3 ± 1.85c	3.26 ± 1.01c	2.35 ± 0.89c	0.72
T_3	34.4 ± 2.75bc	13.0 ± 1.54c	3.68 ± 0.89bc	2.89 ± 0.89bc	0.79
T_4	37.0 ± 4.21b	14.8 ± 2.17b	4.23 ± 0.48b	3.23 ± 0.85b	0.76
T_5	43.0 ± 3.17a	17.9 ± 1.02a	6.96 ± 0.91a	6.16 ± 1.02a	0.88
T_6	36.1 ± 1.75b	14.1 ± 2.03b	4.19 ± 0.81b	3.18 ± 0.79b	0.76

Values were means ± SE. The same lowercase letters in a line indicate non-significant differences among plants in different treatments.
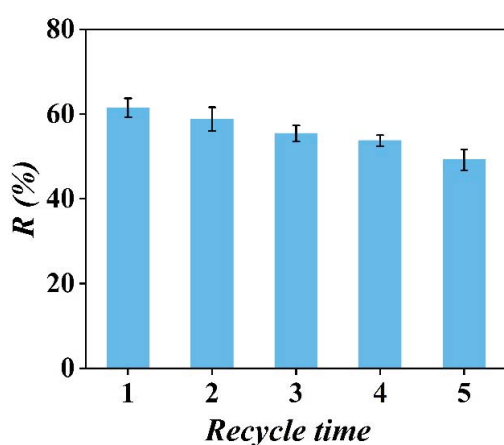

Fig. 11. Repeated reusability of B@M for removal Pb(II) in solution.

while the plant height and root length, aboveground and underground biomass of plants significantly increased ($P < 0.05$). This shows that B@M has a certain ability to remove Pb(II) from wastewater of MCW, and could reduce the stress of heavy metals on plant growth [18,19,45,46], and the effect was much more obvious with the more addition of B@M. The other studies also showed that biochar is a safeguard against the harmful effects of pollutants [17,19].
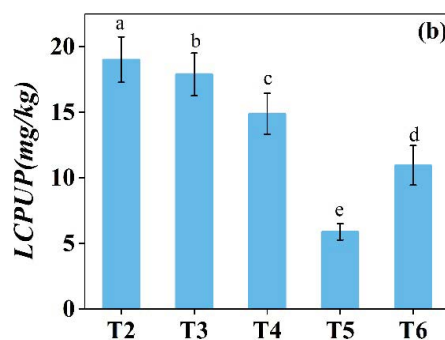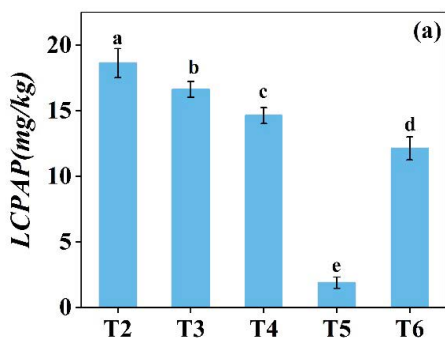
According to the results in Fig. 13, treatment T_2 (without adding B@M) also had 11% removal rate of Pb(II), indicating that plants have certain heavy-metal removal ability in water[18,19,26,45]. However, compared with T_2, the removal rate of Pb(II) in MCW was effectively improved after adding B@M. Meanwhile, with the increasing addition of B@M (T_3, T_4 and T_5), the removal rate of Pb(II) in MCW was significantly increased ($P < 0.05$), with the removal rate of 31.3%, 48.3% and 86.1%, respectively. This showed that adding B@M had a good effect on removing Pb(II) from MCW.

In order to study the reproducibility of B@M, the adsorbed B@M was cleaned with 1 M HNO_3 for several times and then air-dried to continue to be put into the MCW (T_6). Compared with T_4 and T_6, the results showed that the B@M after regeneration had no significant difference in the removal rate of Pb(II) in MCW, which indicated that B@M had good reproducibility. In conclusion, adding B@M had a good effect on removing Pb(II) from MCW. Also, B@M can weaken the stress of Pb(II) on aquatic plants, reduce the content of Pb(II) in plants, and achieve good growth. Therefore, B@M can be used as a new substrate material for CWs and Pb(II) adsorbent.

4. Conclusions

It was found that B@M have a good adsorption capacity of Pb(II) (61.5 mg g⁻¹) because the surface was rough, the functional groups were rich. The adsorption process of
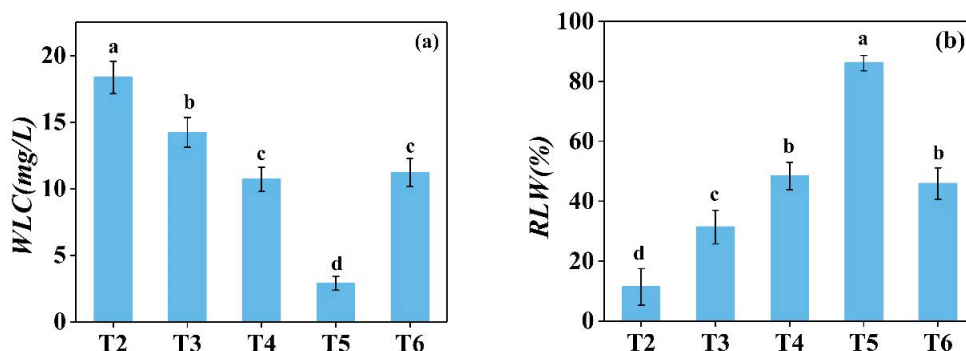

Fig. 12. Pb(II) content in aboveground and underground parts of plants. *Note*: the same lowercase letters in a column indicate non-significant differences among measurements in different treatments. LCPAP: lead content in plant's aboveground part; LCPUP: lead content in plant's underground part.

Fig. 13. Pb(II) concentration and removal rate of water in different treatment devices. *Note*: the same lowercase letters in a column indicate non-significant differences among measurements in different treatments. WLC: water lead concentration; RLW: removal rate of lead in water.

Pb(II) was according to the pseudo-second-order model and Langmuir adsorption model. The results of MCWs showed that with the increased amount of B@M, the removal rate of lead in MCWs increased significantly. It showed that B@M had good reproducibility and can reduce the stress of Pb(II) in plants of MCWs. Therefore, B@M can be used as a new substrate material and heavy metal Pb(II) adsorbent for constructed wetlands.

CRediT authorship contribution statement

Yaohong Zhang and Renrong Liu: Writing - review & editing, Supervision. Liya Tan: Methodology, Writing - original draft, Visualization. Ningcan Yang: Formal analysis, Investigation. kerkula Anna: Validation, Data curation. Hai Wang: Conceptualization, Writing - review & editing, Supervision.

Acknowledgement

References

[1] Y. Liu, C.J. Yan, Z.H. Zhang, H.Q. Wang, S. Zhou, W. Zhou, A comparative study on fly ash, geopolymer and faujasite block for Pb removal from aqueous solution, Fuel, 185 (2016) 181–189.

[2] A.G. Caporale, M. Pigna, A. Sommella, C. Pellegrino, Effect of pruning-derived biochar on heavy metals removal and water dynamics, Biol. Fertil. Soils, 50 (2014) 1211–1222.

[3] P.K. Padmavathiamma, L.Y. Li, Phytoremediation technology: hyper-accumulation metals in plants, Water Air Soil Pollut., 184 (2007) 105–126.

[4] L. Wang, J. Zhang, R. Zhao, Y. Li, C. Li, C.L. Zhang, Adsorption of Pb(II) on activated carbon prepared from *Polygonum orientale* Linn.: kinetics, isotherms, pH, and ionic strength studies, Bioresour. Technol., 101 (2010) 5808–5814.

[5] B.W. Hu, G.H. Chen, C.G. Jin, J. Hu, C.C. Huang, J. Sheng, G.D. Sheng, J.Y. Ma, Y.Y. Huang, Macroscopic and spectroscopic studies of the enhanced scavenging of Cr(VI) and Se(VI) from water by titanate nanotube anchored nanoscale zero-valent iron, J. Hazard. Mater., 336 (2017) 214–221.

[6] N. Yin, K. Wang, L.Z. Wang, Z.Q. Li, Amino-functionalized MOFs combining ceramic membrane ultrafiltration for Pb(II) removal, Chem. Eng. J., 306 (2016) 619–628.

[7] N. Wang, D.X. Yang, X.X. Wang, S.J. Yu, H.Q. Wang, T. Wen, G. Song, Z.M. Yu, X.K. Wang, Highly efficient Pb(II) and Cu(II) removal using hollow Fe$_3$O$_4$@PDA nanoparticles with excellent application capability and reusability, Inorg. Chem. Front., 5 (2018) 2174–2182.

[8] R. Hu, T. Furukawa, Y. Gong, L. Chen, X.K. Wang, X.Y. Tian, M. Nagatsu, Tailoring of Cu@Graphitic carbon nanostructures enables the selective detection of copper ions and highly efficient catalysis of organic pollutants, Adv. Mater. Interfaces, 5 (2018) 1901834, https://doi.org/10.1002/admi.201901834.

[9] X. Liu, J. Sun, X.T. Xu, A. Alsaedi, T. Hayat, J.X. Li, Adsorption and desorption of U(VI) on different-size graphene oxide, Chem. Eng. J., 360 (2019) 941–950.

[10] J. Alvarez, G. Lopez, M. Amutio, J. Bilbao, M. Olazar, Upgrading the rice husk char obtained by flash pyrolysis for the production of amorphous silica and high quality activated carbon, Bioresour. Technol., 170 (2014) 132–137.

[11] B.W. Hu, X.j. Guo, C. Zheng, g. song, D.Y. Chen, Y.L. Zhu, X.F. Song, Y.B. Sun, Plasma-enhanced amidoxime/magnetic graphene oxide for efficient enrichment of U(VI) investigated by EXAFS and modeling techniques, Chem. Eng. J., 357 (2019) 66–74.

[12] G.Q. Tan, Y. Wu, Y. Liu, D. Xiao, Removal of Pb(II) ions from aqueous solution by manganese oxide coated rice straw biochar – a low-cost and highly effective sorbent, J. Taiwan Inst. Chem. Eng., 84 (2018) 85–92.

[13] M.I. Inyang, B. Gao, Y. Yao, Y.W. Xue, A. Zimmerman, A. Mosa, P. Pullammanappallil, Y.S. Ok, X.D. Cao, A review of biochar as a low-cost adsorbent for aqueous heavy metal removal, Crit. Rev. Env. Sci. Technol., 46 (2016) 406–433.

[14] Y. Xie, C.L. Chen, X.M. Ren, X.X. Wang, H.Y. Wang, X.K. Wang, Emerging natural and tailored materials for uranium-contaminated water treatment and environmental remediation, Prog. Mater. Sci., 103 (2019) 180–234.

[15] Y. Yao, B. Gao, J. Fang, M. Zhang, H. Chen, Y.M. Zhou, A.E. Creamer, Y.N. Sun, L.Y. Yang, Characterization and environmental applications of clay–biochar composites, Chem. Eng. J., 242 (2014) 136–143.

[16] H. Wang, N.C. Yang, M.Q. Qiu, Adsorption of Cr(VI) from aqueous solution by biochar-clay derived from clay and peanut shell, J. Inorg. Mater., 35 (2020) 301–308.

[17] A. Mosa, M.F. El-Banna, B. Gao, Biochar filters reduced the toxic effects of nickel on tomato (*Lycopersicon esculentum* L.) grown in nutrient film technique hydroponic system, Chemosphere, 149 (2016) 254–262.

[18] C. Karakaş, D. Özçimen, B. İnan, Potential use of olive stone biochar as a hydroponic growing medium, J. Anal. Appl. Pyrol., 125 (2017) 17–23.

[19] M.F. El-Banna, A. Mosa, B. Gao, X. Yin, Z. Ahmad, H. Wang, Sorption of lead ions onto oxidized bagasse-biochar mitigates Pb-induced oxidative stress on hydroponically grown chicory: experimental observations and mechanisms, Chemosphere, 208 (2018) 887–898.

[20] P. de Rozari, M. Greenway, A.E. Hanandeh, An investigation into the effectiveness of sand media amended with biochar to remove BOD_5, suspended solids and coliforms using wetland mesocosms, Water Sci. Technol., 71 (2015) 1536–1544.

[21] P. Gupta, T.W. Ann, S.M. Lee, Use of biochar to enhance constructed wetland performance in wastewater reclamation, Environ. Eng. Res., 21 (2016) 36–44.

[22] S. Kizito, T. Lv, S.B. Wu, Z. Ajmal, H.Z. Luo, R. Dong, Treatment of anaerobic digested effluent in biochar-packed vertical flow constructed wetland columns: role of media and tidal operation, Sci. Total Environ., 592 (2017) 197–205.

[23] S.B. Lu, X.L. Zhang, J.H. Wang, L. Pei, Impacts of different media on constructed wetlands for rural household sewage treatment, J. Cleaner Prod., 127 (2016) 325–330.

[24] X. Zhou, X. Wang, H. Zhang, H.M. Wu, Enhanced nitrogen removal of low C/N domestic wastewater using a biochar-amended aerated vertical flow constructed wetland, Bioresour. Technol., 241 (2017) 269–275.

[25] X. Zhou, L.X. Jia, C.L. Liang, L.K. Feng, R.G. Wang, H.M. Wu, Simultaneous enhancement of nitrogen removal and nitrous oxide reduction by a saturated biochar-based intermittent aeration vertical flow constructed wetland: effects of influent strength, Chem. Eng. J., 334 (2018) 1842–1850.

[26] X.F. Guo, X.Y. Cui, H.S. Li, Effects of fillers combined with biosorbents on nutrient and heavy metal removal from biogas slurry in constructed wetlands, Sci. Total Environ., 703 (2020) 134788, https://doi.org/10.1016/j.scitotenv.2019.134788.

[27] A. Gedam, R. Donger, Comparative study of sponge gourd derived biochar and activated carbon for bio-sorption and desorption of Pb(II) ions, Mater. Today:. Proc., 18 (2019) 887–900.

[28] A.J. Cooper, The ABC of NFT: Nutrient Film Technique: The World's First Method of Crop Production Without a Solid Rooting Medium, Casper Publications Pty. Ltd., London, 1996.

[29] M.X. Wang, P. Pang, L.K. Koopal, G.H. Qiu, Y. Wang, F. Liu, One-step synthesis of delta-MnO_2 nanoparticles using ascorbic acid and their scavenging properties to Pb(II), Zn(II) and methylene blue, Mater. Chem. Phys., 148 (2014) 1149–1156.

[30] L.J. Dong, J.X. Yang, Y.Y. Mou, G.D. Sheng, L.X. Wang, W.S. Linghu, A.M. Asiri, K.A. Alamry, Effect of various environmental factors on the adsorption of U(VI) onto biochar derived from rice straw, J. Radioanal. Nucl. Chem., 314 (2017) 377–386.

[31] Y. Yao, B. Gao, L.J. Jiang, M.D. Inyang, Y.C. Li, A. Alva, L.Y. Yang, Engineered carbon (biochar) prepared by direct pyrolysis of Mg-accumulated tomato tissues: characterization and phosphate removal potential, Bioresour. Technol., 138 (2013) 8–13.

[32] S.L. Wan, F. He, J.Y. Wu, W.B. Wan, Y.W. Gu, B. Gao, Rapid and highly selective removal of lead from water using graphene oxide-hydrated manganese oxide nanocomposites, J. Hazard. Mater., 314 (2016) 32–40.

[33] N. Zhang, G.-L. Zang, C. Shi, H.-Q. Yu, G.-P. Sheng, A novel adsorbent TEMPO-mediated oxidized cellulose nanofibrils modified with PEI: preparation, characterization, and application for Cu(II) removal, J. Hazard. Mater., 316 (2016) 11–18.

[34] J. Wang, Z.S. Chen, W.Y. Chen, Y.S. Li, Y.C. Wu, J. Hu, A. Alsaedi, N.S. Alharbi, J.F. Dong, W.S. Linghu, Effect of pH, ionic strength, humic substances and temperature on the sorption of Th(IV) onto NKF-6 zeolite, J. Radioanal. Nucl. Chem., 310 (2016) 597–609.

[35] H. Wang, L.Y. Tan, B.W. Hu, M.Q. Qiu, L.P. Liang, L.F. Bao, Y.L. Zhu, G.H. Chen, C.C. Huang, Removal of Cr(VI) from acid mine drainage with clay-biochar composite, Desal. Water Treat., 165 (2019) 212–221.

[36] B.S. Kadu, Y.D. Sathe, A.B. Ingle, R.C. Chikate, K.R. Patil, C.V. Rode, Efficiency and recycling capability of montmorillonite supported Fe-Ni bimetallic nanocomposites towards hexavalent chromium remediation, Appl. Catal., B, 104 (2011) 407–414.

[37] S.Q. Zhang, X. Yang, L. Liu, M.T. Ju, K. Zheng, Adsorption behavior of selective recognition functionalized biochar to Cd(II) in wastewater, Materials, 11 (2018) 299–310.

[38] L.Y. Hao, H.J. Song, L.C. Zhang, X.Y. Wan, Y.R. Tang, Y. Lv, SiO_2/graphene composite for highly selective adsorption of Pb(II) ion, J. Colloid Interface Sci., 369 (2012) 381–387.

[39] X.F. Tan, Y.G. Liu, G.M. Zeng, X. Wang, X.J. Hu, Y.L. Gu, Z.Z. Yang, Application of biochar for the removal of pollutants from aqueous solutions, Chemosphere, 125 (2015) 70–85.

[40] S. Mireles, J.G. Parsons, T. Trad, C.L. Cheng, J. Kang, Lead removal from aqueous solutions using biochars derived from corn stover, orange peel, and pistachio shell, Int. J. Environ. Sci. Technol., 16 (2019) 5817–5826.

[41] R. Sudha, K. Srinivasan, Lead(II) removal from aqueous solution using *Citrus limettioides* peel and its modified form: isotherms, kinetics and thermodynamic studies, Desal. Water Treat., 57 (2016) 13690–13700.

[42] C.Q. Wang, H. Wang, Pb(II) sorption from aqueous solution by novel biochar loaded with nano-particles, Chemosphere, 192 (2017) 1–4.

[43] X. Cui, X. Dai, K. Khan, T. Li, X. Yang, Z. He, Removal of phosphate from aqueous solution using magnesium-alginate/chitosan modified biochar microspheres derived from *Thalia dealbata*, Bioresour. Technol., 218 (2016) 1123–1132.

[44] Y. Li, Z. Yang, Y. Chen, L. Huang, Adsorption, recovery, and regeneration of Cd by magnetic phosphate nanoparticles, Environ. Sci. Pollut. Res., 26 (2019) 17321–17332.

[45] Y.M. Awad, S.-E. Lee, M.B.M. Ahmed, N.T. Vu, M. Farooq, I.S. Kim, H.S. Kim, M. Vithanage, A.R.A. Usman, M. Al-Wabel, E. Meers, E.E. Kwon, Y.S. Ok, Biochar, a potential hydroponic growth substrate, enhances the nutritional status and growth of leafy vegetables, J. Cleaner Prod., 156 (2017) 581–588.

[46] K. Kasak, J. Truu, I. Ostonen, J. Sarjas, K. Oopkaup, P. Paiste, M.K. Vainik, Ü. Mander, M. Truu, Biochar enhances plant growth and nutrient removal in horizontal subsurface flow constructed wetlands, Sci. Total Environ., 639 (2018) 67–74.